Simulating behavior of perfluorooctane sulfonate (PFOS) in the mainstream of a river system with sluice regulations

Guoxiang Han[a,c], Shuai Song[a,c], Yonglong Lu[a,b,c*], Meng Zhang[a,c], Di Du[a,c], Qiang Wu[a,c], Shengjie Yang[a,c], Rui Wang [a,c], Haotian Cui [a,c], Lu Yang [a,c], Ruoyu Mao[a,c], Bin Sun[a,c], Andy Sweetman[d], Yanqi Wu[a,c]

[a] *State Key Laboratory of Urban and Regional Ecology, Research Center for Eco-Environmental Sciences, Chinese Academy of Sciences, Beijing 100085, China*

[b] *Key Laboratory of the Ministry of Education for Coastal Wetland Ecosystems, College of the Environment and Ecology, Xiamen University, Fujian 361102, China*

[c] *University of Chinese Academy of Sciences, Beijing 100049, China*

[d] *Lancaster Environmental Centre, Lancaster University, Lancaster LA1 4YQ, UK*

* Corresponding author:

Yonglong Lu

Tel: 86-10-62917903

Fax: 86-10-62918177

E-mail: yllu@rcees.ac.cn

Abstract: Perfluorooctane sulfonate (PFOS) is a persistent, long-range transport, anionic, and ubiquitous contaminant. Its behavior has attracted wide-ranging scientific and regulatory attention. In this article, the concentrations of PFOS in both freshwater and sediment, and the behavior of PFOS between freshwater and sediment were simulated based on a mass balance approach in the mainstream of Haihe river system combining with sluices and artificial rivers. Annual emission discharged into each river was esitamted and North Canal was the maximum receiver in the study. The simulated concentrations of PFOS in both steady and unsteady states agreed with the measured concentrations in surveys carried out in Nov. 2019, July 2020, Oct. 2020, and June 2021. Every year, approximately 23.2 kg PFOS was discharged into the Bohai Sea with Chaobai New River being the largest contributor for 44%. Moreover, the transport of PFOS in the orginal rivers would be restricted by sluices and replaced by artificial rivers. Monte Carlo analysis showed the model predicting PFOS concentrations in sediment is subject to greater uncertainty than that in freshwater as the former is impacted by more parameters. It provides a scientific basis for local govement to manage and control PFOS in the study area.

Keyword: PFOS, behavior, measured concentrations, mass fluxes, uncertainty

1. Introduction

Perfluorinated products have been widely used in a range of specialized consumer and industrial products as polymers, surfactants, refrigerants, etc. (Zhang et al., 2019; Cui et al., 2020; Dixit et al., 2022; Liagkouridis et al., 2022). Perfluorooctane sulfonate (PFOS, $C_8F_{17}SO_3^-$), as one of the main perfluorinated products, has been identified in a wide range of global media, including the Arctic region (Charbonnet et al., 2021; Charbonnet et al., 2022; Evich et al., 2022; Young et al., 2022). It is released from direct use in products or as an end product of the transformation and metabolism of its precursors (Prevedouros et al., 2006; Paul et al., 2009; Wang et al., 2014b; Wang et al., 2014a; Boucher et al., 2018). Different from polycyclic aromatic hydrocarbons (PAHs) or polychlorinated biphenyls (PCBs), PFOS is a non-volatile surfactant that has required a precursor hypothesis to explain its long-term atmospheric transport (Schenker et al., 2008; Armitage et al., 2009; Cousins et al., 2017; Boucher et al., 2018). Furthermore, there is no evidence that it appears to be subject to any degradation or metabolism, due to its highly stable C-F bonds (Barrett et al., 2021; Ruyle et al., 2021; Hao et al., 2022; Yu et al., 2022).

Previous studies have investigated the behavior of PFOS based on mass balance models, and assumed that the study area was divided into several regions or segments where the compartments were well-mixed or homogeneous (Armitage et al., 2009; Earnshaw et al., 2014; Liu et al., 2015; Cousins et al., 2017; Su et al., 2018). For example, the spatial distribution of PFOS and its concentrations in freshwater and no sediment in the Aire and Calder Rivers were accurately estimated by a model that was

reparametrized from the the Rhine River (Earnshaw et al., 2014). In the previous studies of our research group, the fate of PFOS in the Bohai coastal region of China was simulated with the BETR model and improved BETR-UR, with the Bohai coastal region divided into 56 grid cells (Liu et al., 2015; Su et al., 2018). The trend of PFOS and its volatile precursors with the major production phase-out was modeled and the actual emissions of PFOS and its volatile precursors was capture by CliMoChem where the global is divided into a series of latitudinal bands (Armitage et al., 2009; Cousins et al., 2017).

The mass balance model approach for rivers was proposed (Mackay et al., 1983b) based on model approaches for lakes, with a river being considered as consisting of a series of lakes (Mackay et al., 1983a). It has been widely and successfully applied to research the fate of pollutants in a river, such as PAHs in the Saguenay Fjord, Canada, and PCBs in the Altamaha River (Lun et al., 1998; Kilic and Aral, 2009). It was modified, and then successfully applied to explain the fate of four textile chemicals, silver, and TiO_2 Nanoparticles in the Rhine River (Beck et al., 2000; Scheringer et al., 2000), or PFOS in the Aire and Calder of UK (Earnshaw et al., 2014). G-CIEMS that river was divided according to river node was successful to research the concentration of molinate in Shinano River of Japan (Suzuki et al., 2005).

However, the behavior of PFOS in the mainstream of Haihe River system combined with sluices and artificial rivers, and the effect of sluices and artificial rivers on the behavior of PFOS in rivers hasn't been fully researched by using the mass balance approach for rivers. Although PFOS was unremittingly discharged into the

mainstream of Haihe River system, the concentration of PFOS would sustain a certain range in the natural environment. The Haihe River system is one of the seven major rivers in China and the largest water system in North China, mainly flowing through Beijing and Tianjin, two municipalities directly under the central government in China. There are a large number of PFOS sources that would discharge directly into the Haihe River (Song et al., 2007; Luo et al., 2010; Luo et al., 2011; Wang et al., 2012a). Compared with other rivers, there are lots of sluices and artificial rivers in the mainstream of Haihe River system excavated in both recently and in the past (Wang et al., 2019). It is important to note that there are cleat uncertainties with the mass balance model approach which include simplifications of complex and irreversible problems and unique environmental systems (Meent et al., 1999; Gag et al., 2004; Schenker et al., 2009).

The objectives of this article are to simulate the concentration of PFOS checked by the measured concentrations from Nov. 2019, July 2020, Oct. 2020, and June 2021, explaine why PFOS was unremittingly discharged into rivers but the concentration stay within a certain range instead of rising all the time, illustrate the behavior of PFOS between rivers combined with sluices and artificial rivers and within a river, and analyze the effects of sluices and artificial rivers on the behavior of PFOS and the uncertainty of the river model in the mainstream of Haihe river system. It provides a scientific basis for the local government to manage PFOS in the mainstream of Haihe River system, and also provides a reference for the fate of pollutants in other rivers.

2. Materials and methodology

2.1 Study area

The Haihe River basin (Fig. 1(a)), one of the seven river basins in China, contains Luanhe River water system, Haihe River water system and Tuhai Majia Rivers water system (Fig.1(b)). Among them, its main body is the Haihe River water system.There are a number of water conservancy projects to ensure water supply to Beijing and Tianjin, such as Yongding River Diversion Canal, Ji-Mi Diversion Canal, Water Diversion Project from Luanhe River to Tianjin City, and South-to-North Water Diversion in Haihe Rivers' system. In order to protect Beijing and Tianjin from flood disaster, a number of artificial rivers have been excavated and sluices have been built.

As shown in Fig.1(c), there are 11 rivers in the mainstream of Haihe River water system: Jiyun River, Chaobai River, Chaobai New River, North Canal, Yongding New River, Haihe River, Duliujian River, Yongding River, Daqing River, Ziya River, and South Canal. Among them, North Canal, South Canal, Chaobai New River, Yongding New River, and Duliujian River are artificial rivers. North and South Canals were excavated to transport grain, while others to alleviate flooding. Each of them has a number of hydrological stations, and the majority were constructed with sluices, as shown in Fig.1(c).

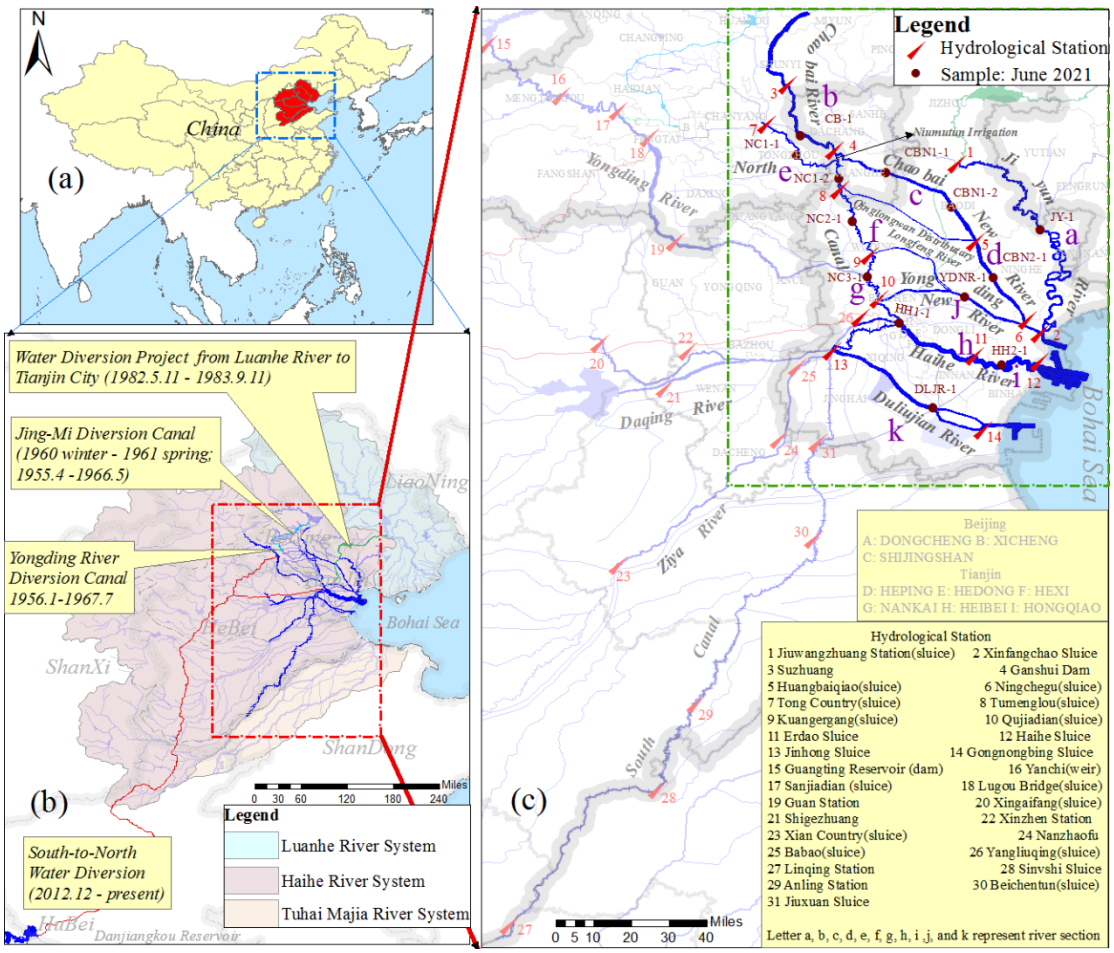

Fig. 1 (a) Location of Haihe River basin; (b) the river water systems in Haihe River basin and major water conservancy projects; (c) Detailed information about the mainstream of the Haihe River system (excluding other artificial rivers), hydrological stations, sampling sites from June 2021, mainstream divisions according to hydrological stations in the model, and districts of Beijing, Tianjin, Langfang and Tangshan.

As shown in *Annual Hydrological Report of China: Hydrological Data of Haihe River Basin in 2017 and 2018*, the Yongding River (Table S1), Daqing River (Table S2, S3, S4 and S5), Ziya River (Table S6), and South River (Table S7) have stopped flowing or only have an occasional flow during wet seasons. In contrast, the other rivers exhibit flows of water due to water conservancy projects, such as the South-to-North Water Diversion. They flow through Beijing, Tianjin, and parts of Langfang and Tangshan (both belong to Hebei province), as shown in Fig. 1(c).

2.2 River model

As shown in Fig. 2, a river can be considered as being divided into a series of sections linked by water flow (Mackay et al., 1983b). Freshwater flows from section $i-1$ to section i, and then from section i to $i+1$. There exist two well-mixed compartments in each section i : freshwater and sediment (RIVM, 1996). Among them, the suspended particulate matter belongs to the freshwater compartment. Pollutants, such as PFOS, would be discharged into freshwater directly not into the sediment. In each section i, pollutants would be adsorbed from freshwater to sediment, whilst also desorbed from sediment to freshwater. The suspended particulate matter with pollutants in freshwater would undergo gravity settlement, while pollutants in sediment would be resuspended to freshwater due to biological activity or currents. Some of the pollutant loadings in sediment could be lost from the freshwater-sediment system via a permanent burial. Generally, pollutants would be degraded or transformed in both freshwater and sediment but PFOS wouldn't (Beck et al., 2000; Scheringer et al., 2000).

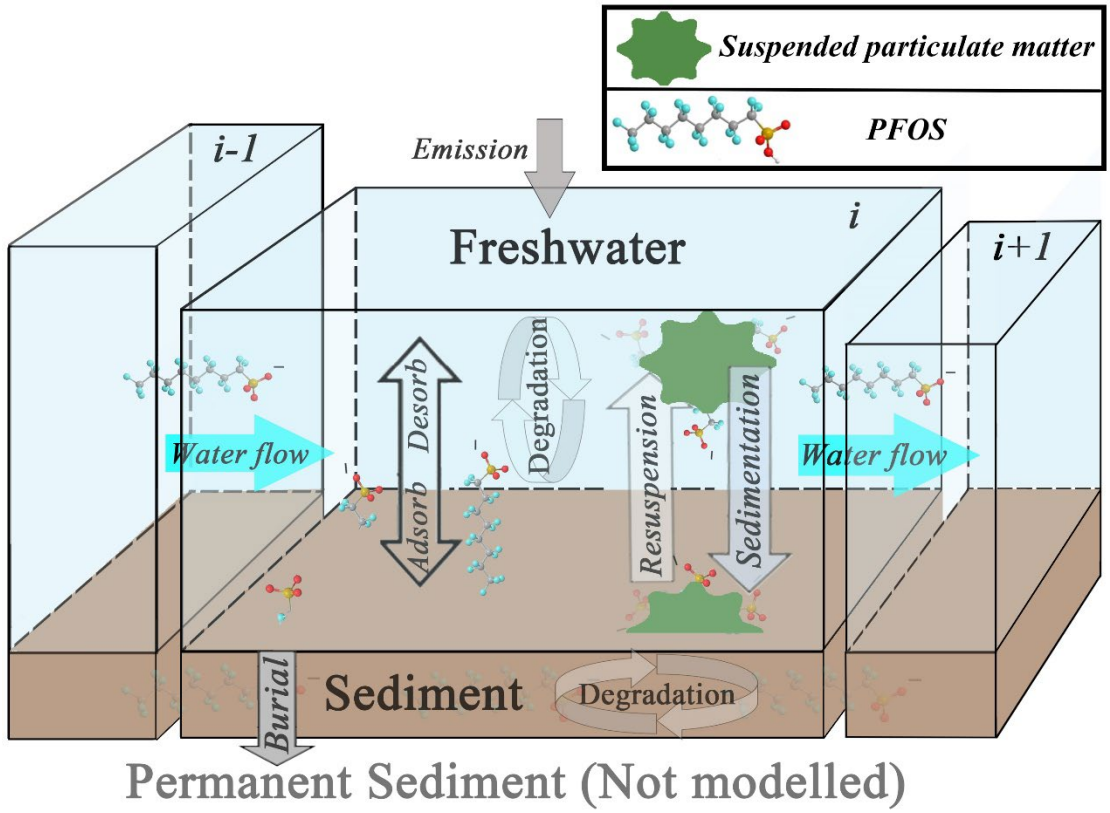

Fig. 2 Each river consists of sections linked by water flow, and the detailed processes between freshwater and sediment in each section.

The mass balance equation of freshwater at section *i* was shown as follow:

$$V_i^{Fw}\frac{dC_i^{Fw}}{dt} = Emis_i^{Fw} + \sum_{i-1=1}^{j} Imp_{i-1\to i}^{Fw} - \sum_{i+1=1}^{k} Exp_{i\to i+1}^{Sed} - Deg_i^{Fw} - Diff_i^{Fw\to Sed} + Diff_i^{Sed\to Fw} - Sed_i^{Fw\to Sed} + Resusp_i^{Sed\to Fw}$$

$i = 1, 2, 3, \ldots, n;$ (1)

The mass balance for sediment at section *i*,

$$V_i^{Sed}\frac{dC_i^{Sed}}{dt} = -Deg_i^{Sed} + Diff_i^{Fw\to Sed} - Diff_i^{Sed\to Fw} + Sed_i^{Fw\to Sed} - Resusp_i^{Sed\to Fw} - Bur_i^{Sed}$$

$i = 1, 2, 3, \ldots, n;$ (2)

where,

V_i^{Fw}: the volume of freshwater at section i;

C_i^{Fw}: the concentration of PFOS in freshwater at section i;

$Emis_i^{Fw}$: the emission of PFOS discharged into freshwater at section i;

$\sum_{i-1=1}^{j} Imp_{i-1\to i}^{Fw}$: impart mass flow from all sections (assuming total j number) $i-1$ to i at section i;

$\sum_{i+1=1}^{k} Exp_{i\to i+1}^{Sed}$: export mass flow from section i to all $i+1$ (assuming total k number) at section i;

Deg^{Fw}: degradation in freshwater at section i;

$Diff_i^{Fw\to Sed}$: adsorb from freshwater to sediment at section i;

$Diff_i^{Sed\to Fw}$: desorb from sediment to freshwater at section i;

C_i^{Sed}: the concentration of PFOS in sediment at section i;

$Sed_i^{Fw\to Sed}$: sedimentation from freshwater to sediment by suspended particular matter at section i;

$Resusp_i^{Sed\to Fw}$: resuspension from sediment to freshwater at section i;

Deg^{Sed}: degradation in sediment at section i;

Bur_i^{Sed}: sediment burial at section i;

The detailed description of $Emis_i^{Fw}$, $Imp_{i-1\to i}^{Fw}$, $Exp_{i\to i+1}^{Fw}$, Deg_i^{Fw}, Deg_i^{Sed}, $Diff_i^{Fw\to Sed}$, $Diff_i^{Sed\to Fw}$, $Sed_i^{Fw\to Sed}$, $Resusp_i^{Sed\to Fw}$, and Bur_i^{Sed} was provided in Supplementary Material S1.

2.3 Parameterization of sections, including estimation of volume and emission

As almost all hydrological stations were built on sluices that impacted the water flow and water level on both sides, compartments between two sluices were considered well-mixed in each section. As shown in Fig. 1(c), the study area was divided into 11 sections according to hydrological stations. The Niumutun Irrigation Channel,

Qinglongwan Distribution, and Longfeng River, artificial rivers, were excavated to help North Canal to flood initially, which has an important function linking these sections.

The Jiyun River was divided into section a from Jiuwangzhuang (sluice) to Xinfangchao Sluice; Chaobai River section b from Suzhuang to Ganshui Dam; Chaobai New River sections c and d from Ganshui Dam to Huangbaiqiao (Sluice) and Huangbaiqiao (sluice) to Ningchegu (sluice); North Canal sections e , f , and g from Tong country to Tumenlou (sluice), Tumenlou (sluice) to Kuangergang (sluice), and from Kuangergang (sluice) to Qujiadian (sluice); Haihe River sections h and i from Qujiandian (sluice), Yangliuqing (sluice) and Jinhong sluice to Erdao sluice, and Erdao sluice to Haihe Sluice; Yongding New River section j from Qujiadian (sluice) to Ningchegu (sluice); and Duliujian River section k from Jinhong Sluice to Gongnongbing Sluice, as shown in Fig.1(c).

The volume of freshwater V_{Fw}^{i} in each section was estimated according to the cross-sectional area (Fig. S2) and the length of sections (Table S8). Generally, water levels were different between inflow and outflow sides of a sluice. If a hydrological station did not give both water levels, the water levels on both sides were assumed equal. Each $Area_i$ between freshwater and sediment was estimated by the length of cross-section (Fig. S2) and section (Table S8). The volume of sediment V_S^i was estimated by $Area_i$ and parameters in Table S9 in each section i.

The emission of PFOS to each section in the mainstream of Haihe River system was estimated using formula (S1), Table S10, S12-S16 and Fig. S3-S11 in Supplementary Material. If a district is served by two rivers, the emission discharged

into one of them was approximately 50%. For example, Baodi and Ninggu is served by Jiyun River and Chaobai New River (Fig. S3, S6). The Binhai district was the result of the merger of Tangu, Hangu, and Dagang in Nov. 2009. The emission of PFOS discharged into Jiyun River (a), Haihe River (i) and Duliujian River (k) from Binhai (Fig. S4) was therefore estimated based the three districts before the merger (Table S13-2).

Tong country station has two sluices: North sluice and Yun sluice. The emission of PFOS discharge from upstream of Chaobai River b and North Canal e was divided according to the discharge into two sluices (Table S16). As the discharge of a number of pollutants has been restricted into Haihe River by controlling sluices and artificial rivers, such as Yongding New River and Duliujian River etc., the emission discharged into section h of Haihe River was approximately estimated by the population of Heping and Hongqiao districts (Fig. S9) timed parameter in Table S10.

2.4 Sampling campaign and chemical analysis

As shown in Fig.1(c), each section has at least one representative sampling site to evaluate the river model performance. Freshwater and sediment were collected separately at each site from Nov. 2019, July 2020, Oct. 2020, and June 2021. The locations of sample sites from June 2021 are shown in Fig. 1(c), and the remaining shown in Fig. S1. Freshwater was stored in 1L clean polypropylene bottles and sediment packed in double-layer polyethylene (PE) bags at -4 temperature before extraction. Freshwater samples were stored at −20 °C and sediment was dried in a room sheltered from light, ground in a mortar and then passed through a 100 mesh sieve, and

packed in PE bags.

The concentrations of linear PFOS in freshwater and sediment samples were measured using previously published methods (Zhang et al., 2019; Wang et al., 2020; Zhang et al., 2021). In brief, 400ml freshwater sample was extracted by cartridge (Oasis WAX) and PFOS in 2g sediment was extracted by acetonitrile and then cleaned up by Supelco ENVI-Carb cartridge and Oasis WAX cartridge. After purification and concentration, the samples were filtered and stored in autosampler vials. The concentrations of PFOS in freshwater and sediment in sample sites were quantified by the Agilent 1290 Infinity HPLC System coupled with an Agilent 6460 Triple Quadrupole LC/MS System (Agilent Technologies, Palo Alto, CA).

A 10-point internal standard calibration curve consisting of 0.01, 0.05, 0.1, 0.5, 1, 5, 10, 100, 500 ng/mL concentration gradients with 5 ng/mL mass-label standard as internal standard was to ensure the accurate quantification of PFOS. The R^2 value of calibration curves of PFOS was greater than 0.99. Then 10 ng native standards of PFOS were added to freshwater and sediment to calculate the matrix spike recoveries (MSRs). The MSRs of PFOS ((mean value ± standard deviation, n = 4) in freshwater and sediment were 105.2 ± 12.5 and 97.5 ± 11, respectively. The limits of quantification of PFOS in freshwater and sediment were 0.06 ng/L and 0.03 ng/g. The limit of detection of PFOS in freshwater and sediment were 0.03 ng/L and 0.01 ng/g, respectively.

2.5 Uncertainty analysis

The simulated concentrations and mass fluxes by mass balances models exhibit uncertainty due to the error of parameter estimations (Meent et al., 1999; Macleod et

al., 2002; Gag et al., 2004). Mento Carlo simulation is an effective method to analyze the produced uncertainty. In our Monte Carlo analysis, the probability distribution of each parameter is assumed to be log-normal distribution, since the values of parameters are positive and the log-normal distribution of parameters is both warranted and advantageous (Mckone, 1994; Slob, 1994; Luo and Yang, 2007). The stochastic data for each parameter was generated from the distribution of parameters with MATLAB, then input into the mass balance model to produce simulated concentrations and uncertainty (Gag et al., 2004; Schenker et al., 2009).

If the logarithmic of a random variable is normal distribution, the random variable is log-normal distribution, shown as follows:

$$Ln(X) \sim N(\mu, \sigma^2) \tag{3}$$

where parameters μ and σ in log-normal distribution are the mean and variance of the corresponding normal distribution on a log scale. Both of them are dimensionless because they are estimated after taking logarithms (Slob, 1994; Mackay et al., 2014; Niwitpong and Somkhuean, 2016). In the original scale, the log-normal distribution is defined by the population median (M) and the population coefficient of variation (CV) that is the arithmetic standard deviation divided by its arithmetic mean (Mckone, 1994), as follows:

$$M = b^{\mu} \tag{4}$$

$$CV = \sqrt{b^{\sigma^2 lnb} - 1} \tag{5}$$

The 95% interval confidence can be shown as follows:

$$Prob\left\{\frac{M}{k} < X < M \times k\right\} = 95\% \tag{6}$$

and k is the dispersion factor, as follows

$$k = e^{1.96\sqrt{\ln(CV^2+1)}} \quad (7)$$

Among, population (Table S12-S15) and rate of water flow (Table S17) were assumed with a fixed log-transformed CV value 5% (Xu et al., 2006). And the assumed CV of other parameters were shown in Table S17.

3. Results and discussion

3.1 Estimated emissions

The divisions of PFOS potentially discharged into Jiyun River are shown in Fig S3, S4; and for the Chaobai River in Fig. S5, S6; the Chaobai New River in Fig. S6, S7; the North Canal in Fig. S5, S7 - S9; the Haihe River in Fig. S4, S10; the Yongding New River in Fig. S8; and the Duliujian River in Fig. S4, S11. The annual emissions of PFOS were approximately 1.8, 5.0, 1.4, 6.7, 3.5, 2.2, and 2.9 kg in the Jiyun River, Chaobai River, Chaobai New River, North Canal, Haihe River, Yongding New River, and Duliujian River, respectively, and the maximum receiver was North Canal, as shown in Fig.5. For Jiyun River, Chaobai River, North Canal, Haihe River, and Duliujian River, the mass fluxes of PFOS transported by water flow from upstream were also taken part of their emission (Fig.5).

In the whole mainstream of Haihe River system, the total annual emission of PFOS was approximately 23.6 kg. Among them, the top three rivers with the highest contribution to the emissions of PFOS were 28% for North Canal, 21% for Chaobai River, and 15% for Haihe River, as North Canal and Chaobai River were affected by Beijing City (Zhang et al., 2016; Wang et al., 2019), and Haihe River by Tianjin City.

The emission contributed to the Jiyun river accounted for 8% of total emission, which is consistent with its distance far from Beijing and Tianjin shown in Fig.1(c).

3.2 Comparison of measured concentrations and predicted values at a steady state

The predicted concentrations of PFOS in freshwater and sediment under steady-state conditions simulated by the river model shown in section 2.1 with parameters in Table S8-S16, were compared to the measured data collected in Nov. 2019, July 2020, Oct. 2020, and June 2021 (some only in June 2021) using the method described in section 2.4. Fig. 3(a-k) shows the simulated results versus the four measured concentrations in sections $a-k$, suggesting that the simulated concentrations agreed well with the measurements.

The predicted concentrations were lower than the maximum of the corresponding measured concentration and greater than the minimum of the corresponding measured ones in both compartments at almost all sections (Fig. 3a1-3k2). For example, in section a of Jiyun River, the predicted freshwater concentration was 7.84 ng/L lower than 8.95 ng/L (sampling date: Oct. 2020) and higher than 1.65 ng/L (June 2021) (Fig. 3a1). Although there was only a sampling site in June 2021 in sections b, f, and j, it is not significantly different. The predicted concentrations of PFOS in freshwater were more accurate than for those in sediment, especially in sections d, and g, as the predicted concentration of PFOS in sediment was affected by more parameters than that in fresh water, such as organic carbon content of sediment, density of solid phase, etc.

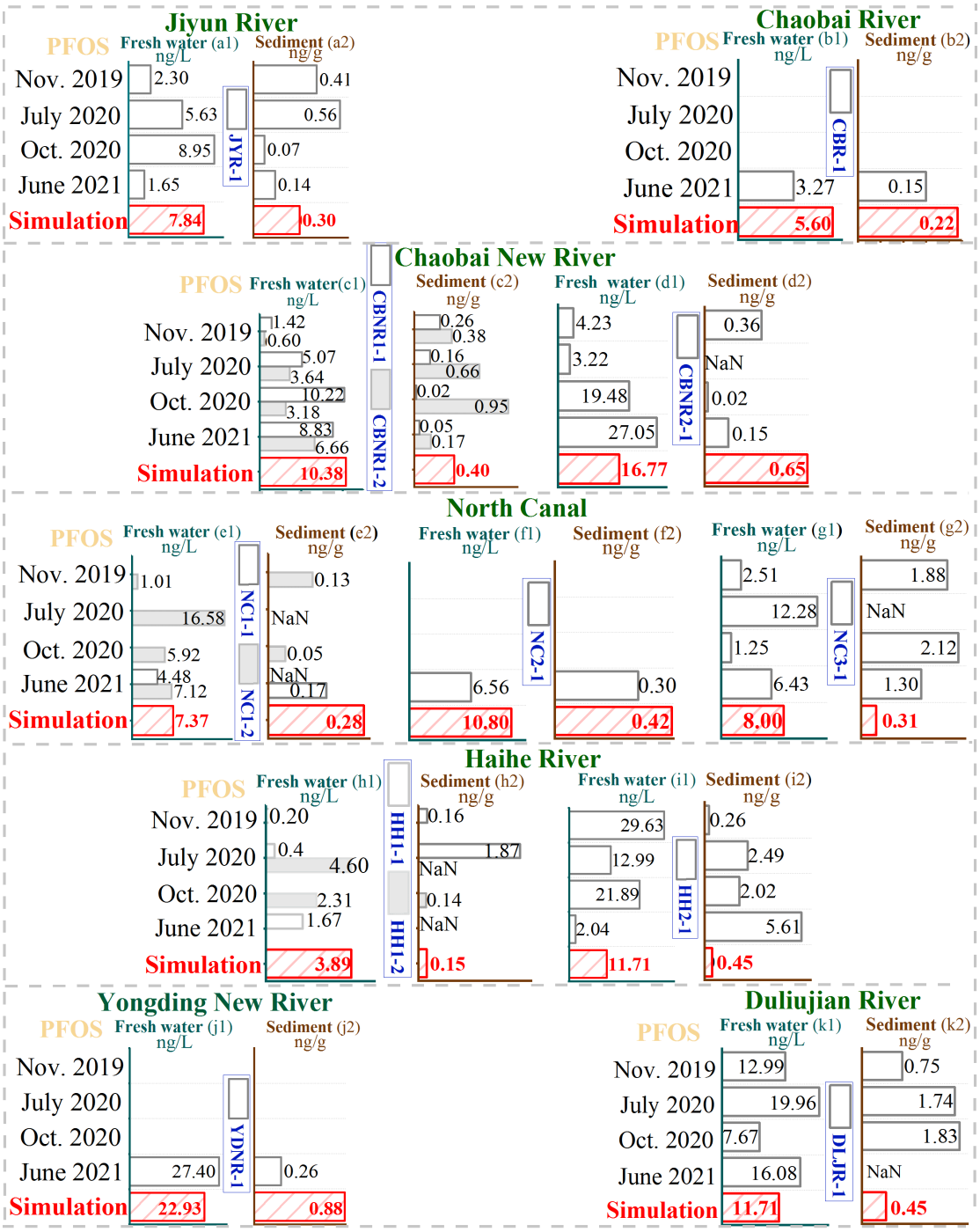

Fig. 3 The concentration of PFOS in freshwater (left) and sediment (right) measured in Nov. 2019, July 2020, Oct. 2020, and June 2021 and the simulation values under steady state in Jiyun River (a1, and a2), Chaibai River (b1, and b2), Chaibai New River (c1, c2, d1, and d2), North Canal (e1, e2, f1, f2, g1, and g2), Haihe River (h1, h2, i1, and i2), Yongding New River (j1, and j2), and Duliujian River (k1, and k2) (some sections only have sample sites from June 2021).

The predicted concentrations were 7.37, 10.50, and 8.00 ng/L in fresh water in

North Canal, which was consistent with 9.44 and 11.02 ng/L from the high flow period reported by (Zhang et al., 2016). The predicted concentrations of PFOS in freshwater were 7.84, 22.93 and 11.71 ng/L in the Jiyun River, Yongding New River, and Duliujian River, respectively, and were significantly higher than the measured concentrations of 0.74, 2.4 and 1.7 ng/L in 2012 (Wang et al., 2012a), respectively. The predicted sediment concentrations were 0.88 and 0.45 ng/g in Yongding New River and Duliujian River, respectively, which was almost equal to 0.94 and 0.53 ng/g measured in 2012 by (Wang et al., 2012b).

Predicted concentrations were 3.89 and 11.71 ng/L in freshwater, and 0.15 and 0.45 ng/g in sediment in the Haihe River, which agreed well with that measured data ranging from 1.11 to 7.22 ng/L and 0.062 to 0.79 ng/g reported by (Pan et al., 2011), with 2.02-7.62 ng/L and 1.76 - 7.32 ng/g reported by (Li et al., 2011), and 1.5 and 10 ng/L (Wang et al., 2012a) and 1.2 and 4.3 ng/g by (Wang et al., 2012b), from separate studies. These comparisons showed that the concnetraions of PFOS in Haihe River haven't changed much over the years, revealing Haihe River was protected and the discharge of PFOS was restricted by local government.

3.3 **Simulated concentrations of PFOS with an unsteady-state**

In the natural environment, emission, volumes of freshwater and sediment, parameters of PFOS, and parameters of river change over time. As they are affected by lots of factors, such as season, temperature, rainfall, etc., the concentration of PFOS in both compartments will respond as a function of time. Assuming that the parameters are fixed for simplification and taking the results of steady-state (Fig.3) as the initial

condition of the unsteady state, the concentrations of PFOS in freshwater and sediment under unsteady-state conditions have been estimated by the method in section 2.2. The results in both compartments with the unsteady-state were shown in Fig. 4(a-k).

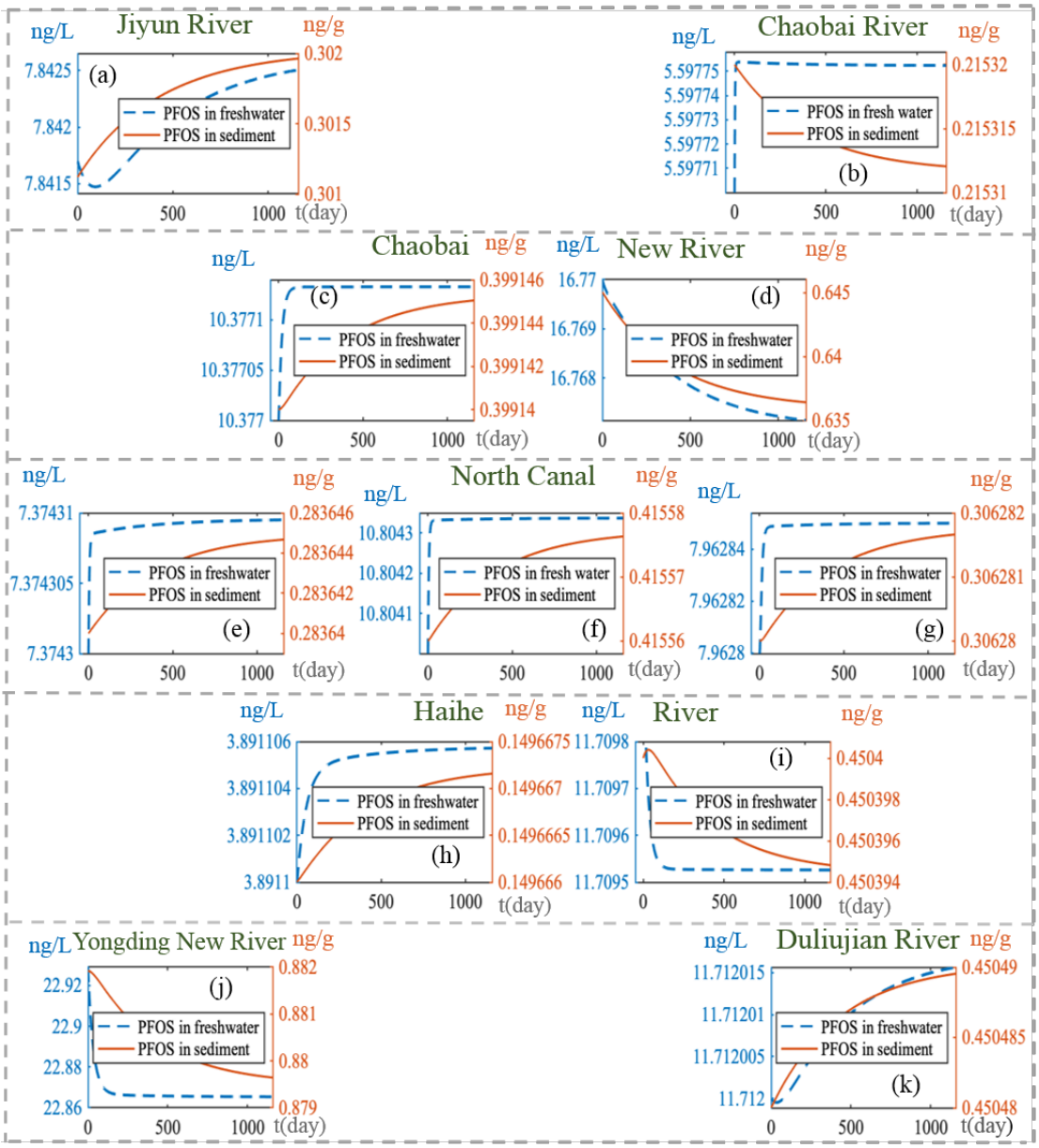

Fig. 4 The results of PFOS with the unsteady state in freshwater (left) and sediment (right) in Jiyun River (a), Chaibai River (b), Chaibai New River (c and d), North Canal (e, f, and g), Haihe River (h and i), Yongding New River (j), and Duliujian River (k).

As shown in Fig. 4(a-k), the concentration curves of PFOS in freshwater and

sediment would tend to a certain value when the exchanged of PFOS reached thermodynamic equilibrium in the freshwater-sediment system. Under thermodynamic equilibrium, the concentration of PFOS in both compartments would be sutained at a certain value, although PFOS was unremittingly discharged into fresh water, imported and outported by water flow between sections, exchanged between compartments in every section, and buried in sediment. The results with unsteady state explain why PFOS was discharged into the mainstream of Haihe River system but the concenraion of PFOS sustained a certain range and wouldn't increase all the time in the natural environment.

3.4 The mass fluxes of PFOS in the mainstream of Haihe River system

The annual mass fluxes of PFOS in the mainstream of the Haihe River system were estimated by formulations (1, 2), and (S1-S12), shown in Fig.5. The Chaobai River, North Canal, Chaobai New River, Yongding New River, HaiHe River, and Duliujian River as well as Niumutun Irrigation Channel, Qinglongwan Distribution, and Longfeng River form a complex structure, while Jiyun River forms an independent, and simple water system by itself.

Under dynamic equilibrium between fresh water and sediment, the mass fluxes of adsorption were almost equal to those of the corresponding desorption in each river as they were derived by differences in chemical potentials in freshwater and sediment (RIVM, 1996), approximately from 109 ~ 797 g in one of the rivers, shown in Fig.5. Nevertheless, the values of sedimentation were totally unequal to the corresponding value of resuspension in one of rivers in the mainstream, as both processes are the single

direction (RIVM, 1996). Each year, approximately 0.613 ~ 3.79 g PFOS were removed from freshwater to sediment, while approximately 0.0774 ~ 0.479 g PFOS were resuspended from sediment to fresh water in one of them. The mass fluxes of degradation in both freshwater and sediment were 0 kg in all rivers, as the highly stable C-F bond in PFOS.

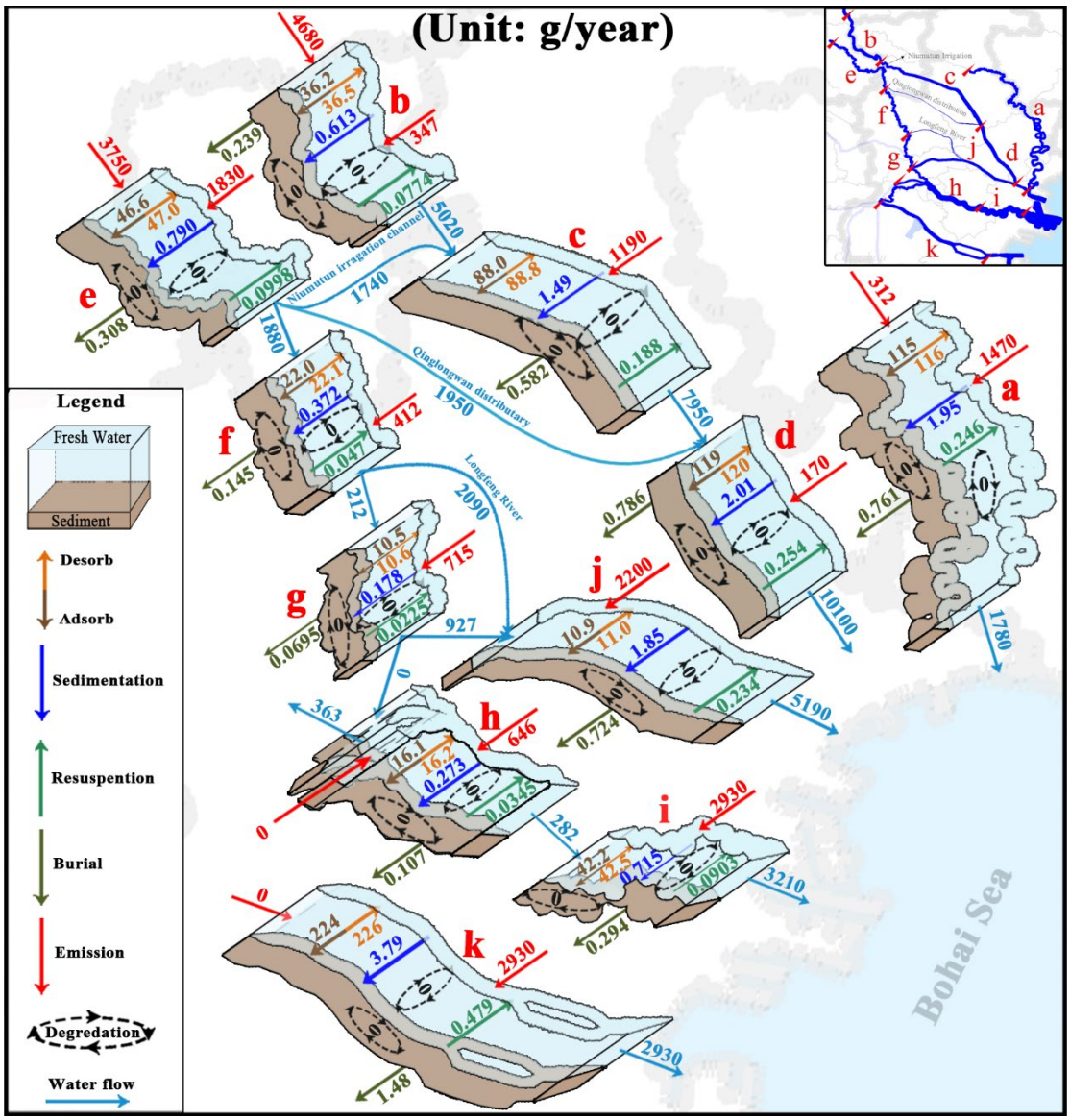

Fig. 5 The mass fluxes of PFOS in each section ins Jiyun River (a), Chaibai River (b), Chaibai New River (c & d), North Canal (e & f & g), Haihe River (h & i), Yongding New River (j), and Duliujian River (k), and between sections. The Niumutun Irrigation Channel, Qinglongwan Distribution and Longfeng River have a function to link rivers.

A total of 5.48 g per year PFOS were estimated to be buried in sediment in the mainstream of Haihe River system. Among them, the top two rivers that contributed the highest burial were Duliiujian River (27%) and Chaobai New River (25%), as their area between sediment and freshwater was greater than the others. The rank of rivers based on the mass value of sediment burial was Duliujian River > Chaobai New River > Jiyun River > Yongding New River > North Canal > Haihe River > Chaobai River.

Every year, approximately 23 kg of PFOS was estimated to have been discharged from Jiyun River, Chaobai New River, Haihe River, and Duliujian River to the Bohai Sea. The most important contributor to the total was the Chaobai New River at 44% of the total, the second was Yongding New River at 22%, the third was Haihe River at 14%, the fourth was Duliujian River at 13%, and the last was Jiyun River at 8%. As the Chaobai New River is responsible for the sewage discharge from Beijing, it has the maximum value of PFOS discharged into the Bohai Sea. The mass balance approach for river has been used to estimated an annual mass discharged of PFOS the Aire and Calder rivers were from 215 to 310 kg in UK (Earnshaw et al., 2014). The mass fluxes of PFOS deposition to the Arctic were approximately 2.0 to 200kg/year over the period 1996-2000 range by CliMoChem (Armitage et al., 2009).

For comparison, a mass flux of PFOS was estimated to be 26 kg/year from the Yonding River, Haihe River, and Duliujian River to Bohai sea by (Zhou et al., 2018) which was comparable to this study; emissions from Jinyun River, Yongding New River, Haihe River, and Duliujian River to the Bohai sea were 10 kg/year, which was lower

than the results from this study as emissions of PFOS were lower a decade ago (Wang et al., 2012a). In comparison, the summary of PFOS discharged into the Bohai Sea from rivers in LiaoNing, HeBei, Tianjin City, and Shandong was estimated to be from 80.0 to 80.5 kg/year which was higher than the results from this study (Chen et al., 2016).

3.5 Sluices and artificial rivers

Sluices and artificial rivers played an important role in the transport of PFOS in the mainstream of Haihe River system. Water flow is restricted by the presence of sluices which would be replaced by the flow from an artificial river. A representative sluice is Qujiandian (North Sluice) which totally restricts the transport of the PFOS from North Canal to Haihe River to protect the health of Haihe River (0 kg shown in Fig. 5), while pollutants are entirely transported from North Canal to Yongding New River through Quijiandian (Yongxin Sluice).

Representative artificial rivers are Nummutun Irrigation Channel, Qinglongwan Distribution, and Longfeng River. Approximately 31% and 35% of the PFOS in the original North Canal (section e) was replaced by Numutun Irrigation Channel, and Qinglongwan Distribution through Numutun Sluice and Tumenlou (Qing Sluice), respectively. In combination, they approximately replaced 66% of the function of North River (section e). Approximately 91% of the PFOS in the original North Canal in section g was replaced by Longfeng River through Kangergang (Jiezhi Sluice).

Although Chaobai New River, Yongding New River, and Duliujian River have been parts of the mainstream of Haihe River system, they are actually artificial rivers that replace the function of Haihe River. Approximately 46%, 24%, and 16% of the

total PFOS transported in the original Haihe River were replaced by Chaobai New River, Yongding New River and Duliujian River, respectively. Of course, North Canal, an ancient artificial river, played an important role in transporting PFOS in the mainstream of Haihe River system, accounting for approximately 28% of the PFOS in the mainstream.

3.6 Uncertainty of model estimates

The predicted concentrations of PFOS in the two compartments are shown in Fig.6 after 100000 simulations by Monte Carlo using MATLAB with the assumed distribution of paramaters in section 2.5 and Table S17. The probability distribution of simulated PFOS concentration in both freshwater and sediment followed the log-normal distribution, and the values of their parameters μ and σ in each section were shown in Fig.6(a-k) with the median values, 95% confidence intervals, and coefficients of variance.

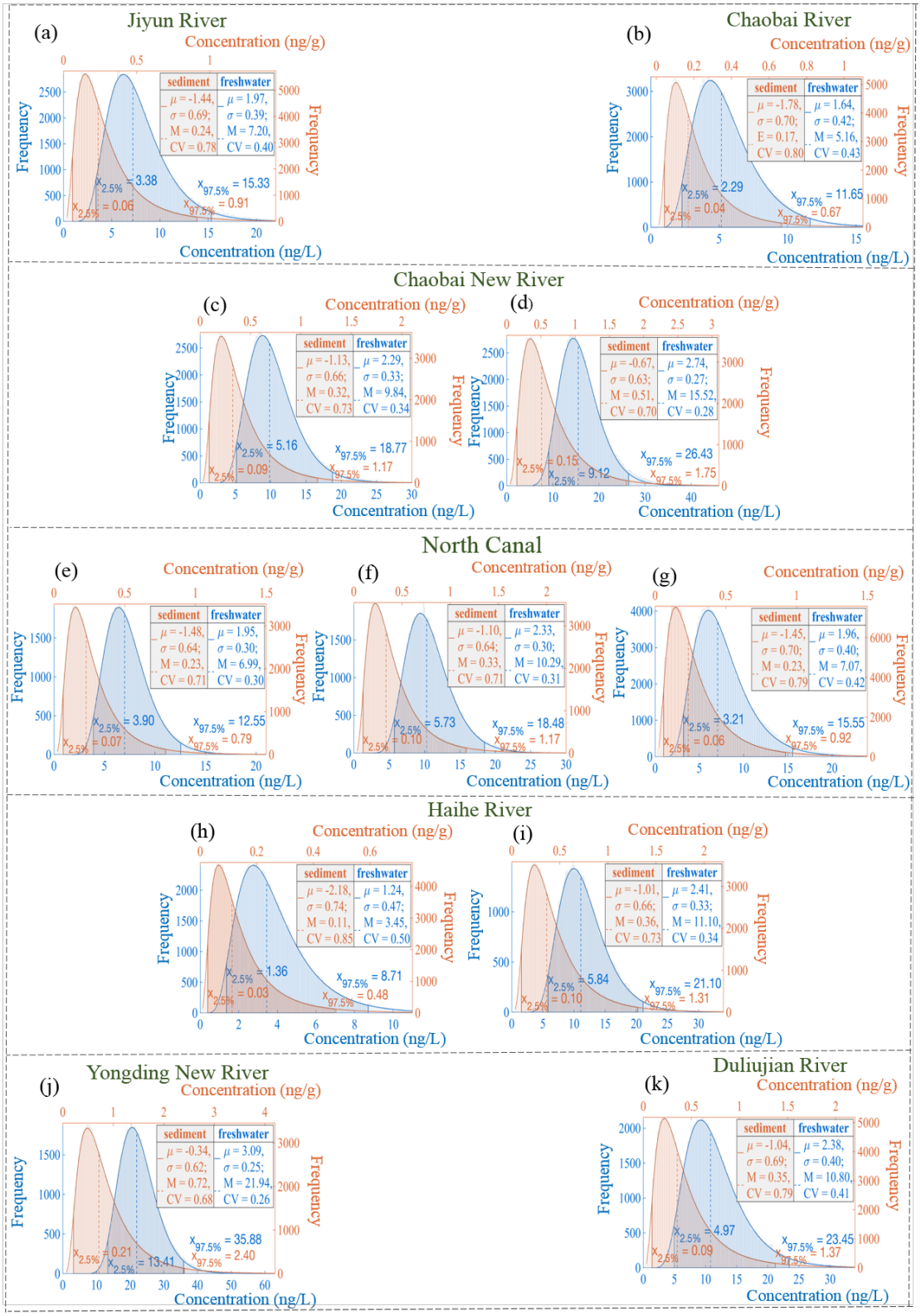

Fig. 6 Both probability distribution of PFOS in freshwater (left) and sediment (right) with Monte Carlo in Jiyun River (a), Chaobai River (b), Chaobai New River (c and d), North Canal (e, f and g), Haihe River (h and i),Yongding New River (j), and Duliujian River (k), respectively.μ and σ are parameters of lognormal distribution ($Y = \ln(X) \sim N(\mu, \sigma^2)$). Capital M is median value, and CV is coefficient of variable.

Among, the simulated concentration of PFOS in compartments in sections 3.2 and 3.3 were within the 95% interval confidence of the corresponding compartments, and most of the measured concentrations in section 3.2 fall into 95% interval confidence. The median value of PFOS concentration in freshwater and sediment in each section was slightly lower than that corresponding one simulated with both steady-state and unsteady-state in sections 3.2 and 3.3, showing the structure of the model was stable to a certain extent and no individual parameter was identified as having a significant impact on the predictions.

The values of CV in freshwater ranged from 0.25 to 0.50, while those in sediment ranged from 0.69 to 0.86 in Fig. 6(a-k). The former values were significantly lower than those in the corresponding one showing there existed more uncertainty in sediment than that in freshwater, as the simulated concentrations in sediment were propagated by more parameters, such as density of sediment (ρ) (Gag et al., 2004). That was consistent with the results that the predicted concentrations of PFOS in freshwater were more accurate than for those in sediment in section 3.1. Additionally, this study has not considered that PFOS is degraded from its precursors (Wang et al., 2014b; Wang et al., 2014a).

4. Conclusion

The mainstream of Haihe River system was analyzed and divided according to hydrological data and hydrological stations. The annual emissions were estimated in each river based on the division, and the top three rivers with the highest contribution were identified as North Canal (28%), Chaobai River (21%), and Haihe (15%). The predicted concentration of PFOS with both steady state and unsteady state based on

mass balance equations were agreed with the measured concentration of PFOS at sampling sites from Nov. 2019, July 2020, Oct. 2020, and June 2021. The unsteady state results explain why PFOS was discahged but the coencentration woul sustain a certain range instead of increasing all the time.

The transport of PFOS between rivers combined with sluices and artificial rivers, and transport and transformation within a river between freshwater and sediment were illustrated. Among, total mass fluxes of 23.2 kg and 5.48 g PFOS were estimated to flow into the Bohai Sea and were buried in the mainstream of Haihe River system, respectively. And sluice would restrict the transport of PFOS in rivers, such as Qujiandian (North sluice); artificial rivers, including some become part of the mainstram of Haihe water system, would replaced the funcation of orginal rivers to transporting PFOS. The uncertainty analysis estimated the distribution and its parameters, median value, 95% interval confidence and CV value, indicating there was more uncertainty in sediment than freshwater.

References:

Armitage, J. M., Schenker, U., Scheringer, M., Martin, J. W., Macleod, M., Cousins, I. T. 2009. Modeling the Global Fate and Transport of Perfluorooctane Sulfonate (PFOS) and Precursor Compounds in Relation to Temporal Trends in Wildlife Exposure. Environmental Science & Technology. 43(24): 9274-9280.

Barrett, H., Du, X., Houde, M., Lair, S., Verreault, J., Peng, H. 2021. Suspect and Nontarget Screening Revealed Class-Specific Temporal Trends (2000–2017) of Poly- and Perfluoroalkyl Substances in St. Lawrence Beluga Whales. Environmental Science & Technology. 55(3): 1659-1671.

Beck, A., Scheringer, M., Hungerbuhler, K. 2000. Fate modelling within LCA. International Journal of Life Cycle Assessment. 5(6): 335-344.

Boucher, Justin, M., Cousins, Ian, T., Scheringer, Martin, Hungerbuhler, Konrad, Wang, Zhanyun. 2018. Toward a Comprehensive Global Emission Inventory of C4-C10 Perfluoroalkanesulfonic Acids (PFSAs) and Related Precursors: Focus on the Life Cycle of C6- and C10-Based Products. Environmental Science & Technology Letters. 6(1): 1-7.

Charbonnet, J. A., McDonough, C. A., Xiao, F., Schwichtenberg, T., Cao, D., Kaserzon, S., Thomas, K. V., Dewapriya, P., Place, B. J., Schymanski, E. L., Field, J. A., Helbling, D. E., Higgins, C. P. 2022. Communicating Confidence of Per- and Polyfluoroalkyl Substance Identification via High-Resolution Mass Spectrometry. Environmental Science & Technology Letters.

Charbonnet, J. A., Rodowa, A. E., Joseph, N. T., Guelfo, J. L., Field, J. A., Jones, G. D., Higgins, C. P., Helbling, D. E., Houtz, E. F. 2021. Environmental Source Tracking of Per- and Polyfluoroalkyl Substances within a Forensic Context: Current and Future Techniques. Environmental Science & Technology. 55(11): 7237-7245.

Chen, H., Wang, X., Zhang, C., Sun, R., He, X. 2016. Occurrence and inputs of perfluoroalkyl substances (PFASs) from rivers and drain outlets to the Bohai Sea, China. Environmental Pollution. 221: 234.

Cousins, Ian, T., Hungerbuhler, Konrad, Boucher, Justin, M., Wang, Zhanyun. 2017. Toward a Comprehensive Global Emission Inventory of C4-C10 Perfluoroalkanesulfonic Acids (PFSAs) and Related Precursors: Focus on the Life Cycle of C8-Based Products and Ongoing Industrial Transition. Environmental Science & Technology. 51: 4482-4493.

Cui, J., Gao, P., Deng, Y. 2020. Destruction of Per- and Polyfluoroalkyl Substances (PFAS) with Advanced Reduction Processes (ARPs): A Critical Review. Environmental Science & Technology. 54(7): 3752-3766.

Dixit, F., Munoz, G., Mirzaei, M., Barbeau, B., Liu, J., Duy, S. V., Sauvé, S., Kandasubramanian, B., Mohseni, M. 2022. Removal of Zwitterionic PFAS by MXenes: Comparisons with Anionic, Nonionic, and PFAS-Specific Resins. Environmental Science & Technology. 56(10): 6212-6222.

Earnshaw, M. R., Paul, A. G., Loos, R., Tavazzi, S., Paracchini, B., Scheringer, M., Hungerbühler, K., Jones, K. C., Sweetman, A. J. 2014. Comparing measured and modelled PFOS concentrations in a UK freshwater catchment and estimating emission rates. Environment International. 70: 25-31.

Evich, M. G., Davis, M. J. B., McCord, J. P., Acrey, B., Awkerman, J. A., Knappe, D. R. U., Lindstrom, A. B., Speth, T. F., Tebes-Stevens, C., Strynar, M. J., Wang, Z., Weber, E. J., Henderson, W. M., Washington, J. W. 2022. Per- and polyfluoroalkyl substances in the environment.

Science. 375(6580): eabg9065.
Gag, H., SHU FULIU, X. U., Jr., R. M. C., Cao, J., Bengang, L. I., Liu, W., Wang, X., Jianying, H. U., Shen, W., Qin, B. 2004. Multimedia Fate Model for Hexachlorocyclohexane in Tianjin, China. Environmental Science & Technology. 38(7): 2126-2132.
Hao, S., Choi, Y. J., Deeb, R. A., Strathmann, T. J., Higgins, C. P. 2022. Application of Hydrothermal Alkaline Treatment for Destruction of Per- and Polyfluoroalkyl Substances in Contaminated Groundwater and Soil. Environmental Science & Technology. 56(10): 6647-6657.
Kilic, S. G., Aral, M. M. 2009. A fugacity based continuous and dynamic fate and transport model for river networks and its application to Altamaha River. Science of the Total Environment. 407(12): 3855-3866.
Li, F., Sun, H., Hao, Z., He, N., Zhao, L., Tao, Z., Sun, T. 2011. Perfluorinated compounds in Haihe River and Dagu Drainage Canal in Tianjin, China. Chemosphere. 84(2): 265-271.
Liagkouridis, I., Awad, R., Schellenberger, S., Plassmann, M. M., Cousins, I. T., Benskin, J. P. 2022. Combined Use of Total Fluorine and Oxidative Fingerprinting for Quantitative Determination of Side-Chain Fluorinated Polymers in Textiles. Environmental Science & Technology Letters. 9(1): 30-36.
Liu, S., Lu, Y., Xie, S., Wang, T., Jones, K. C., Sweetman, A. J. 2015. Exploring the fate, transport and risk of Perfluorooctane Sulfonate (PFOS) in a coastal region of China using a multimedia model. Environment International. 85: 15-26.
Lun, R., Lee, K., De Marco, L., Nalewajko, C., Mackay, D. 1998. A model of the fate of polycyclic aromatic hydrocarbons in the Saguenay Fjord, Canada. Environmental Toxicology & Chemistry. 17(2): 333-341.
Luo, Y., Mao, D., Rysz, M., Zhou, Q., Alvarez, P. 2010. Trends in Antibiotic Resistance Genes Occurrence in the Haihe River, China. Environmental Science & Technology. 44(19): 7220-7225.
Luo, Y., Xu, L., Rysz, M., Wang, Y., Zhang, H., Alvarez, P. 2011. Occurrence and Transport of Tetracycline, Sulfonamide, Quinolone, and Macrolide Antibiotics in the Haihe River Basin, China. Environmental Science & Technology. 45(5): 1827-1833.
Luo, Y., Yang, X. 2007. A multimedia environmental model of chemical distribution: Fate, transport, and uncertainty analysis. Chemosphere. 66(8): 1396-1407.
Mackay, D., Hughes, L., Powell, D. E., Kim, J. 2014. An updated Quantitative Water Air Sediment Interaction (QWASI) model for evaluating chemical fate and input parameter sensitivities in aquatic systems: Application to D5 (decamethylcyclopentasiloxane) and PCB-180 in two lakes. Chemosphere. 111: 359-365.
Mackay, D., Paterson, S., Joy, M. 1983a. A quantitative water, air, sediment interaction(QWASI) fugacity model for describing the fate of chemicals in lakes. Chemosphere. 981-997.
Mackay, D., Paterson, S., Joy, M. 1983b. A quantitative water, air, sediment interaction(QWASI) fugacity model for describing the fate of chemicals in river. Chemosphere. 1193-1208.
Macleod, M., Fraser, A. J., Mackay, D. 2002. Evaluating and expressing the propagation of uncertainty in chemical fate and bioaccumulation models. Environmental Toxicology & Chemistry. 21(4): 700-709.
Mckone, T. E. 1994. Uncertainty and Variability in Human Exposures to Soil Contaminants Through Home-Grown Food: A Monte Carlo Assessment. Risk Analysis. 14(4): 449-463.

Meent, V. D., D., Etienne, R., S., Ragas, A., M. J., Willemsen, F., H. 1999. Assessing model uncertainty for environmental decision making: a case study of the coherence of independently derived environmental quality objectives for air and water. Environmental Toxicology & Chemistry. 18(8): 1856–1867.

Niwitpong, S. A., Somkhuean, R. 2016. Confidence intervals for the median of lognormal distribution with restricted parameter mean. International Journal of Mathematics Trends and Technology. 29(1): 21-27.

Pan, Y., Shi, Y., Wang, J., Jin, X., Cai, Y. 2011. Pilot Investigation of Perfluorinated Compounds in River Water, Sediment, Soil and Fish in Tianjin, China. Bulletin of Environmental Contamination and Toxicology. 87(2): 152-157.

Paul, A. G., Jones, K. C., Sweetman, A. J. 2009. A first global production, emission, and environmental inventory for perfluorooctane sulfonate. Environmental Science & Technology. 43(2): 386-392.

Prevedouros, K., Cousins, I. T., Buck, R. C., Korzeniowski, S. H. 2006. Sources, Fate and Transport of Perfluorocarboxylates. Environmental Science & Technology. 37(11): 32-44.

RIVM. 1996. SimpleBox 2.0: a nested multimedia fate model for evaluating the environmental fate of chemicals. Report no. 719101029. National Institute for Public Health and the Environment, Bilthoven, The Netherlands.

Ruyle, B. J., Thackray, C. P., McCord, J. P., Strynar, M. J., Mauge-Lewis, K. A., Fenton, S. E., Sunderland, E. M. 2021. Reconstructing the Composition of Per- and Polyfluoroalkyl Substances in Contemporary Aqueous Film-Forming Foams. Environmental Science & Technology Letters. 8(1): 59-65.

Schenker, U., Scheringer, M., Macleod, M., Martin, J. W., Cousins, I. T., Hungerbuhler, K. 2008. Contribution of volatile precursor substances to the flux of perfluorooctanoate to the arctic. Environmental Science & Technology. 42(10): 3710-3716.

Schenker, U., Scheringer, M., Sohn, M. D., Maddalena, R. L., Mckone, T. E., Hungerbuehler, K. 2009. Using Information on Uncertainty to Improve Environmental Fate Modeling: A Case Study on DDT. Environmental Science & Technology. 43(1): 128-134.

Scheringer, M., Halder, D., Hungerbuhler, K. 2000. Comparing the environmental performance of fluorescent whitening agents with peroxide bleaching of mechanical pulp. Journal of Industrial Ecology. 3(4): 77-95.

Slob, W. 1994. Uncertainty Analysis in Multiplicative Models. Risk Analysis. 14: 571-576.

Song, Y. U., Shao, M., Liu, Y., Sihua, L. U., Kuster, W., Goldan, P., Xie, S. 2007. Source apportionment of ambient volatile organic compounds in Beijing. Environmental Science & Technology. 41(12): 4348-4353.

Su, C., Lu, Y., Wang, T., Lu, X., Song, S., Li, L., Khan, K., Wang, C., Liang, R. 2018. Dynamic multimedia fate simulation of Perfluorooctane Sulfonate (PFOS) from 1981 to 2050 in the urbanizing Bohai Rim of China. Environmental Pollution. 235: 235-244.

Suzuki, N., Murasawa, K., Nansai, K., Sakurai, T., Matsuhashi, K., Moriguchi, Y., Tanabe, K., Nakasugi, O., MORITA, M., Morita, M. 2005. Development of Geo-Referenced Environmental Fate Model (G-CIEMS) for Chemical Contaminants Based on GIS (Geographic Information System (In Janpanese). Journal of Environmental Chemistry. 15(2): 385-395.

Wang, G., Yan, D., Pan, T., He, X., Qi, J., Ren, M., Zhao, L., Wang, F., Zhang, Z., Jiang, X. 2019. Study on Technical Schemes for Major Pollutants Emission Reduction in Beijing North Canal

River Basin Based on Watershed Water Quality Target Management. Journal of Water Resource and Protection. 11(11): 1327-1350.

Wang, P., Lu, Y., Su, H., Su, C., Jenkins, A. 2020. Managing health risks of perfluoroalkyl acids in aquatic food from a river-estuary-sea environment affected by fluorochemical industry. Environment International. 138: 105621.

Wang, T., Khim, J. S., Chen, C., Naile, J. E., Giesy, J. P. 2012a. Perfluorinated compounds in surface waters from Northern China: Comparison to level of industrialization. Environment International. 42(1): 37-46.

Wang, T., Lu, Y., Chen, C., Naile, J. E., Khim, J. S., Giesy, J. P. 2012b. Perfluorinated compounds in a coastal industrial area of Tianjin, China. Environmental Geochemistry and Health. 34(3): 301-311.

Wang, Z., Cousins, I. T., Scheringer, M., Buck, R. C., Hungerbühler, K. 2014a. Global emission inventories for C4–C14 perfluoroalkyl carboxylic acid (PFCA) homologues from 1951 to 2030, Part I: production and emissions from quantifiable sources. Environment International. 62-75.

Wang, Z., Cousins, I. T., Scheringer, M., Buck, R. C., Hungerbühler, K. 2014b. Global emission inventories for C4–C14 perfluoroalkyl carboxylic acid (PFCA) homologues from 1951 to 2030, part II: The remaining pieces of the puzzle. Environment International. 69: 166-176.

Xu, S., Liu, W., Tao, S. 2006. Emission of polycyclic aromatic hydrocarbons in China. Environmental Science & Technology. 40(3): 702-708.

Young, R. B., Pica, N. E., Sharifan, H., Chen, H., Roth, H. K., Blakney, G. T., Borch, T., Higgins, C. P., Kornuc, J. J., McKenna, A. M., Blotevogel, J. 2022. PFAS Analysis with Ultrahigh Resolution 21T FT-ICR MS: Suspect and Nontargeted Screening with Unrivaled Mass Resolving Power and Accuracy. Environmental Science & Technology. 56(4): 2455-2465.

Yu, Y., Che, S., Ren, C., Jin, B., Tian, Z., Liu, J., Men, Y. 2022. Microbial Defluorination of Unsaturated Per- and Polyfluorinated Carboxylic Acids under Anaerobic and Aerobic Conditions: A Structure Specificity Study. Environmental Science & Technology. 56(8): 4894-4904.

Zhang, M., Wang, P., Lu, Y., Lu, X., Sarvajayakesavalu, S. 2019. Bioaccumulation and human exposure of perfluoroalkyl acids (PFAAs) in vegetables from the largest vegetable production base of China. Environment International. 135: 37-47.

Zhang, M., Wang, P., Lu, Y., Shi, Y., Wang, C., Sun, B., Li, X., Song, S., Yu, M. 2021. Transport and environmental risks of perfluoroalkyl acids in a large irrigation and drainage system for agricultural production. Environment International. 157: 106856.

Zhang, Y., Wang, B., Wang, W., Li, W., Deng, S., Wang, Y., Yu, G. 2016. Occurrence and source apportionment of Per-and poly-fluorinated compounds (PFCs) in North Canal Basin, Beijing. Scientific Reports. 6(1): 1-9.

Zhou, Yunqiao, Wang, Tieyu, Qifeng, Pei, Lei, Chen, Shuqin, Zhang. 2018. Spatial and vertical variations of perfluoroalkyl acids (PFAAs) in the Bohai and Yellow Seas: Bridging the gap between riverine sources and marine sinks. Environmental Pollution. 238: 111-120.